



Performance Enhancement of a Transonic Axial Flow Compressor with Circumferential Casing Grooves to Improve the Stall Margin

N. Ahmad, J. Bin[†], Z. Qun, S. Abdu Ahmad and H. Fawzy

College of Power and Energy Engineering, Harbin Engineering University, Harbin 150001, China

[†]Corresponding Author Email: jiangbin_hrbeu@163.com

(Received February 10, 2019; accepted April 27, 2019)

ABSTRACT

The stability range of the gas turbine engine compressors is being challenged in the modern days due to the intention of increasing per stage maximum loading. Casing treatment has been widely adopted as a realistic passive flow control means to improve the stall margin with a slight decrease of efficiency at the same time by various grooves of which shape (location, angles and so on) has a significant influence on controlling effect. However, the influence of some details in grooves is ignored in most of the case that may impact the specific flow field in the groove. A research on the impact of chamfer and fillet corners on the performance of casing treatment was proceeded by numerical simulation in this paper. The performance of different models of grooves on NASA Rotor 37 was investigated by discretizing 3D RANS based on finite volume method. Firstly, steady simulations were performed on NASA rotor 37 for validation. The CFD results and experimental data for adiabatic efficiency and pressure ratio were in good agreement. According to convergence criteria, the initiation of the stall was predicted. Few numbers of circumferential grooves casing treatment (CGCT) models have been proposed and tested numerically. Rectangular CGCT shape and smooth wall casing performances were analyzed. Moreover, the highest adiabatic efficiencies and stall margins of smooth wall casing, rectangular grooves and rectangular grooves with chamfer and fillet corners shapes models were compared to evaluate the influence of the shape of grooves on the stability and performance on axial flow compressor. The rectangular circumferential casing grooves and rectangular grooves with chamfer and fillet corners enhanced significantly stall margin and an operational range of the transonic axial flow compressor but adiabatic efficiency was slightly decreased.

Keywords: Numerical simulation; Axial compressor; Circumferential grooves; Adiabatic efficiency; Stall margin.

NOMENCLATURE

CFD	Computational Fluid Dynamics				
CGCT	Circumferential Grooves Casing Treatment			γ	ratio of specific heat
				η	adiabatic efficiency
EXP	Experiment				
LE	Leading Edge				Subscripts
\dot{m}	mass flow rate			SW	Smooth Wall
PR	Total Pressure Ratio			Ave	average
SM	Stall Margin			Peak	adiabatic efficiency at peak
SS	Suction Surface			Max	maximum
PS	Pressure Surface			Min	minimum
P_t	total pressure			Stall	near stall point
RANS	Reynolds Averaged Navier Stokes			In	inlet
T_t	total temperature			Out	outlet
TE	Trailing Edge				
y^+	non-dimensional wall distance				

1. INTRODUCTION

Axial flow compressor is very important for the design of gas turbines, such as the aerospace engine, marine engine, and jet engine. Axial flow compressors have high reliability, flexible operation and also high performance. Due to low aspect ratio and high mass flow percentage operating in turbomachinery axial flow compressor is an important part of the gas turbine. Because of surge and stall, severe vibration may experience in the axial compressor. Due to this reason, it creates problems in the stability and also minimizes the performance of the compressor. In order to grasp the maximum advantage, the range of the flow should be increased in the operating region between the stability of low flow limit and high compressor efficiency. Many researchers have done numerous efforts in divulging the mechanism of the stall and surge to increase the axial compressor operating range by numerical analysis and experimental techniques. The primary factor for axial flow compressor instability is TLV near the shroud region. TLV is controlled by the passive method of casing treatment to improve the operating stability of the compressor, but the efficiency penalty is also accompanied by the casing treatment. Several techniques have been proposed to increase the stall margin for the compressor. Bailey (1972) tested solid casing wall with different circumferential casing grooves experimentally. For the grooved configurations, they had used Aluminum removable casing inserts in their modifications. The number of grooves, location and depth were changed for circumferential grooves in their research. Their results showed that the application of grooves in compressor improve stability and stall margin. Suder *et al.* (1994) revealed that the shock and tip leakage vortex interaction produced a large region for fluid that had a very low speed which directly goes downstream of both interactions. The flow of the blockage could displace all over in the endwall region which produced a large adverse pressure gradient. Schlechtriem *et al.* (1997) and Yamada *et al.* (2007) reported that due to breaking down of blade tip leakage vortex (BTLV) at the leading-edge stall was elicited. Wilke *et al.* (2002) carried out numerical investigation on the front stage of HPC to find the influence of CGCT. They reported that the BTLV extension was suppressed by the CGCT and stall margin could also improve with grooves. Rabe *et al.* (2002) experimentally and numerically investigated to study the influence of depth and number of CGCT on performance and stall margin. In another study, Hah *et al.* (2004) showed that the vortex cessation for the rotor to swept forward does not happen essentially if the operating condition of the compressor was stalled, which produced a large adverse pressure gradient. Beheshti *et al.* (2004) performed parametric research to study the stability and performance of a NASA rotor 37 by circumferential casing grooves with respect to change in the tip clearance. The results showed that the abrasion coating casing treatment in a transonic axial flow compressor was capable of improving the stability and performance. Shabbir *et al.* (2005)

worked on low-speed rotor to check the CGCT physical mechanism with the analysis of the budget of axial momentum equation. Huang *et al.* (2008) worked on the circumferential grooves' width and depth casing treatment to improve the stall margin and performance using numerical analysis and they proposed that mechanism of the stall was significantly affected by clearance tip. Khan *et al.* (2011) worked on the CGCT, tip recess and combined model of both to evaluate the behavior of stall of NASA rotor 37. They suggested that the combined model was more marginal to stall improvement. Houghton *et al.* (2011) performed experimental work on a single groove to change the axial position of the groove to assess the efficiency, stability and stall margin. They reported that the grooves interaction in forward and aft position were different. Kim *et al.* (2012) investigated the CGCT with various shapes to improve the performance and stall margin. They suggested that CGCT applications gave substantial improvement with a small drop in efficiency. Sakuma *et al.* (2014) investigate NASA rotor 37 with a single groove and changed different locations axially. They revealed that the TLF momentum and tip loading was minimized by CGCT. The effect of CGCT with three different methods on the axial compressor with low speed was experimentally investigated by Rolfes *et al.* (2015). They found that the compressor operating range was increased by CGCT. Lang *et al.* (2017) investigated the install behavior by performing multi-passage unsteady simulations on transonic axial flow compressor. They found that a tip leakage breakdown occurred at stall due to an interaction between the detached shock wave and tip leakage. They also found that The TLV went downstream moved up and the new vortex was formed by TLV. In the tip region, the blockage occurred due to these vortices. Dinh *et al.* (2017) researched on non-axisymmetric CGCT with the combined effect of air flow injection on NASA rotor 37. They suggested that non-axisymmetric CGCT with the injection of air greatly improved the stable range and stall margin of the compressor but a little decreased in efficiency. Mirzabozorg *et al.* (2017) worked on NASA rotor 37 to investigate the width and locations effect on the stability of the transonic compressor. They reported that with the installation of narrow grooves the efficiency was slightly decreased while with large width the efficiency was more decreased. Hah (2018) investigated the influence of ACG on low speed one and a half stage axial flow compressor to study the SM and efficiency. He proposed that with the installation of the ACG stall margin was much improved without any penalty of efficiency. Song *et al.* (2018) researched numerically on multiple grooves and installed the grooves in different axial location. Lean and sweep variations were also introduced and then determined the influenced with grooves. They reported that using grooves with lean and sweep variations, the stall margin and performance of the compressor substantially improved. Though the previous researchers' emphasis on grooves types, shapes, depths and but ignoring some actual structures of chamfer and fillet corners.

Table 1 Design Specification of NASA Rotor 37 (Dunham, 1998)

Number of rotor blades	36
Design mass flow rate (kg/s)	20.19
Rotational speed (rpm)	17188.7
Rotor tip solidity	1.29
Total pressure ratio	2.106
Rotor inlet hub-to-tip diameter ratio	0.7
Rotor tip relative inlet Mach number	1.48
Rotor hub relative inlet Mach number	1.13
Rotor blade aspect ratio	1.19
Tip clearance (design) (mm)	0.356 (at 47 % span)
Mass flow choking (kg/s)	20.93
Reference temperature (K)	288.15
Rotor polytropic efficiency	0.889
Reference pressure (Pa)	101325
Tip speed (m/s)	454.136
Blade airfoil sections	Multiple-Circular-Arc

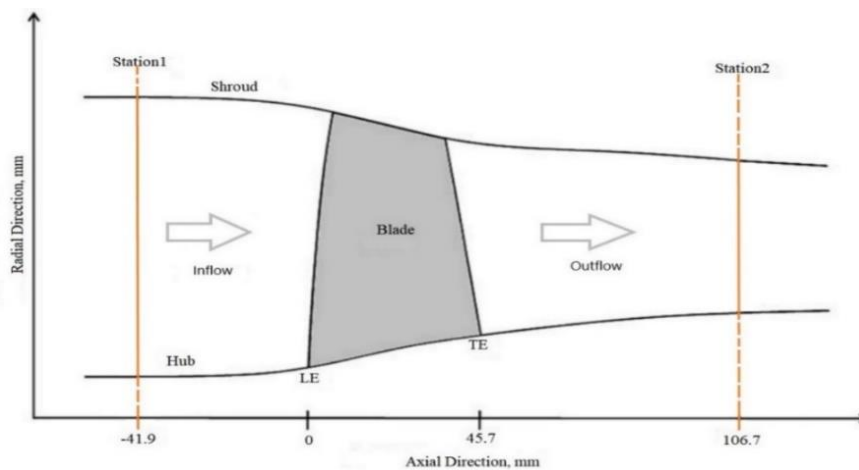


Fig. 1. NASA rotor 37 Meridional view.

The main purpose of this research is to numerically study the influence of circumferential casing grooves, rectangular shape and rectangular shapes with chamfer and fillet corners on the axial flow compressor performance using 3D RANS equations. The adiabatic efficiency and stall margins of various chamfer and fillet shapes were also compared with normal casing and experimental work to discover the effect of rectangular shape and rectangular shapes with chamfer and fillet corners grooves.

2. DESIGN SPECIFICATIONS FOR NASA ROTOR 37

A high-pressure ratio NASA rotor 37 transonic axial flow compressor is selected for this study. The complete design specifications are given in Table 1 which were taken from the AGARD Advisory report by Dunham (1998). The number of blades of this

rotor is 36 and the rotational speed by which the rotor operates is 17188.7 revolution per minute. The total pressure ratio of this rotor is 2.106 and the polytropic efficiency is 88.9 % at the design mass flow is 20.19Kg/s. The choked mass flow of the rotor is 20.93 kg/s and 0.925 (normalized mass flow) which is close to the stall point of the choked mass flow. The tip clearance of the rotor is 0.356 mm (47 % span). The blade airfoil sections of NASA rotor 37 is explained by multiple circular arc (MCA).

NASA rotor 37 meridional plane is depicted in Fig. 1. At station 1 (inlet) the flow parameters like total temperature and total pressure are measured related to mass flow rate and station 2 (outlet) is depicted in this figure. The distance between the blade leading edge and station 1 is -41.9 mm upstream while station 2 is located 106.7 mm downstream from blade trailing edge close to the hub.

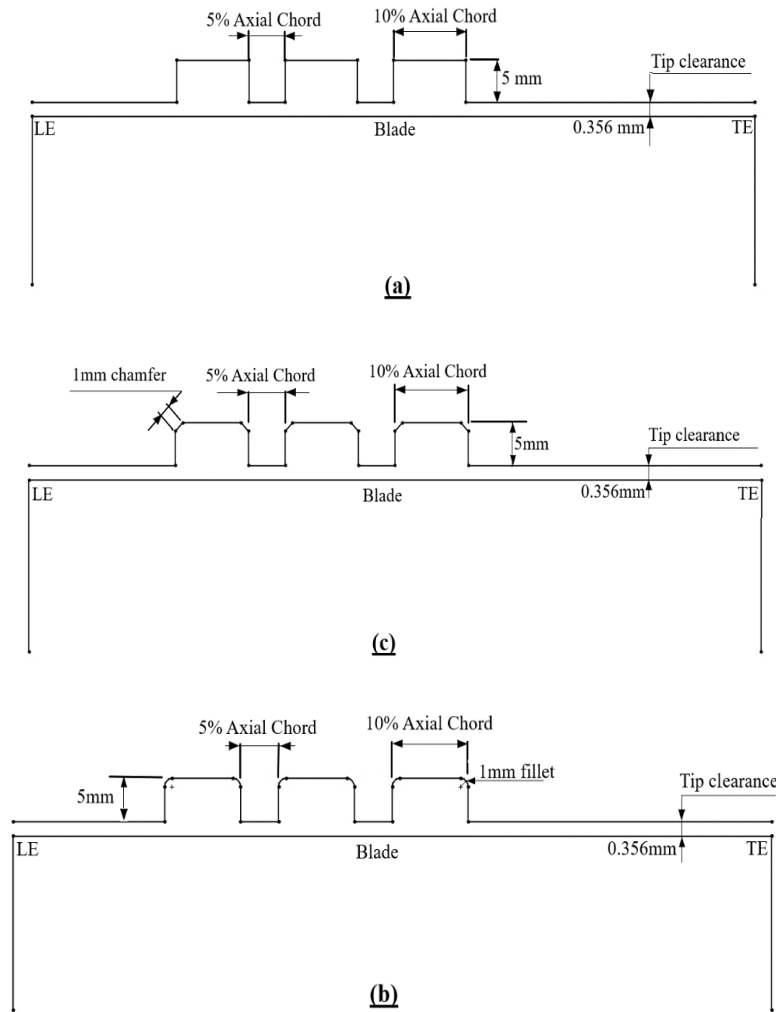


Fig. 2. CGCT different Profiles (a) model 1, (b) model 2 and (c) model 3.

3. DESIGN AND ILLUSTRATION OF CGCT

For this research, three dissimilar circumferential profiles of grooves were designed for NASA rotor 37 to ameliorate the performance and stability of the rotor, as depicted in Fig. 2. The performances and stabilities of each model were compared with one another and also with smooth casing. Each model consists of three grooves and the grooves were located from eighteen percent to fifty-eight percent of the blade chord. The model 1 circumferential grooves shape was rectangular and the depth of the grooves was 5mm. The width of each groove consists of ten percent axial chord tip and the gap between two grooves was five percent of the axial chord tip. Previous Researchers (Huang *et al.*, 2008; Kim *et al.*, 2012) researched on the rectangular grooves depth, tip clearance and width to find the effects of these factors on stall margin. They revealed that using CGCT could enhance the performance and stable range of the axial flow compressor. So, model 1 is the basic model of this research that was used to explore the casing grooves effects for axial flow

compressor performance. Model 2 and model 3 are depicted in Figs. 2(b) and (c) and the models had fillet and chamfer shapes. The depth of the grooves in each model was 5 mm and the length of the fillet and chamfer in model 2 and 3 was 1 mm each.

4. NUMERICAL METHOD

ANSYS (17, 2017) was used for axial flow compressor along with CGCT by applying steady governing 3D flow analysis for this research. With the help of the finite volume method RANS three-dimensional equation was discretized. NUMECA IGG (2009) CFX (Pre-solver manager and post) were used for the creation of blade profile, generate meshing, the definition of boundary conditions, numerical method and post-processing. Fluid domain and circumferential casing grooves were created in CREO (PTC Creo Elements Pro 5.0 M220 Win64) and design modeler and mesh was generated in ICEM- CFD correspondingly. The one passage computational domain was used in this research for the axial flow compressor assuming periodic flow in the circumferential direction of

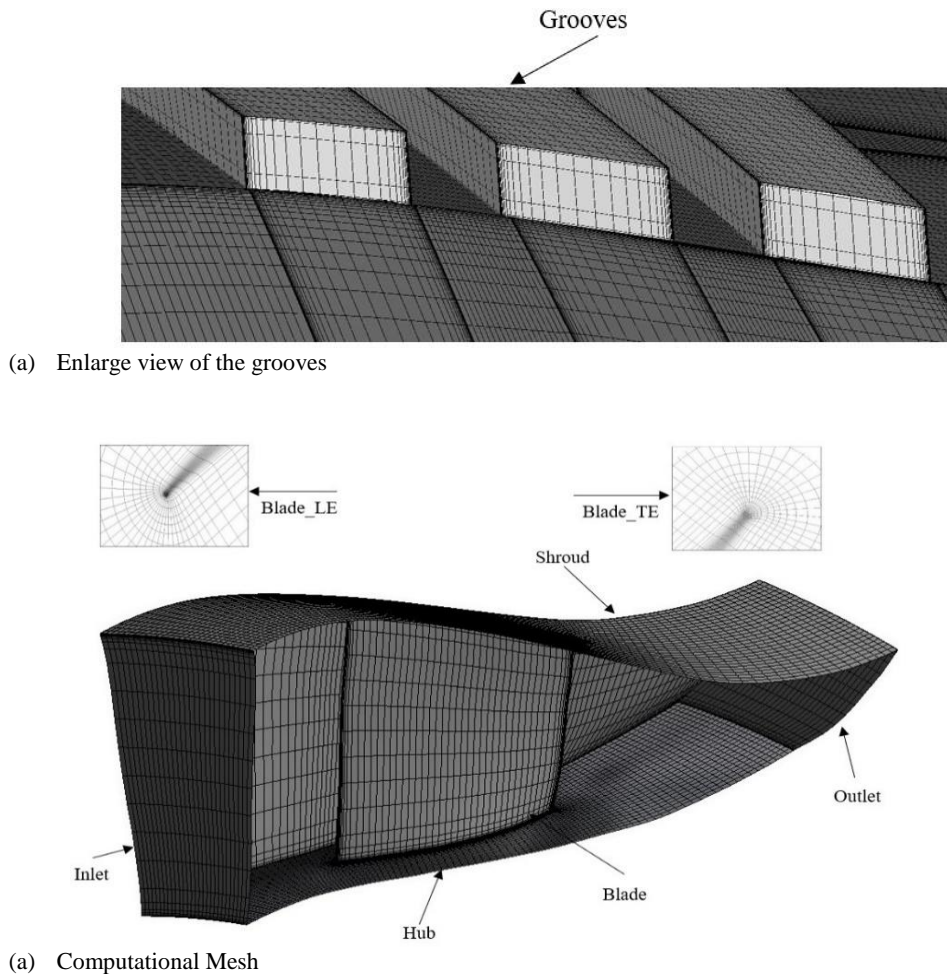


Fig. 3. NASA Rotor 37 computational mesh.

rotation among two adjacent rotor blades. A structure block grids were created in the flow passage for the axial compressor rotor. The number of mesh computation is depicted in Fig. 3. H-O-H topology was used for structure meshing. O type grids were constructed at the blade leading and trailing edge and H type grids were constructed for the region of the main flow. The grids of H type were also used for the grooves. The number of grids for the inlet block was $17 \times 21 \times 40$ while the number of grids for outlet block was $17 \times 25 \times 40$. The total number of nodes for this research were 4.45×10^5 and the number of grids for each groove block was $20 \times 30 \times 60$. The number of grids for three cases between the pressure at mid-span and streamwise location is depicted in Fig. 3. The number of grids for the three models were 222000, 445000 and 780000. It could be seen in Figs. 4 and 5 when the number of grids were changed from 445000 to 780000, there was a little change occurred in the pattern. In addition, computational grids effect on compressor characteristic map is showed in Fig. 4 for 222000, 445000 and 780000 grids. As seen in the figure the adiabatic efficiency and total pressure ratio were less changed when the grid size was changed between 445000 and 780000. So, the case having grids number of 445000 were selected for this research. The SST turbulence model was used for

this numerical computation. According to [Kim *et al.*, \(2012\)](#); [Mirzabozorg *et al.* \(2017\)](#) the SST model is appropriate for the separation of adverse pressure gradient flow analysis. The shear stress of wall treatment depends upon the precision of turbulent flow for the numerical calculation. The minimum y^+ wall unit for the first grid layer was strictly set below two to seizure the shear stress of the wall accurately. Table 2 summarized minimum, average and maximum values of y^+ for the suction side, pressure side, hub and shroud of the compressor rotor. Ideal air gas was considered working fluid for this research work. At inlet total pressure of 1 atm and total temperature, 288.15k were fixed. The interface of the blade passage was set as periodic. Adiabatic with no slip wall and smooth wall for the rotor blade were considered in boundary details.

Radial equilibrium condition was imposed at the outlet. Back pressure was increased at the outlet by imposing the condition of radial equilibrium to calculate the radial distribution for static pressure at the outlet. The back pressure was increased by 100 Pa in each case near the stall region. So, the point near to stall was considered the last steady point. The grooves and the blade passage were connected with GGI method. The same convergence criteria is used

in this research work which was suggested by Huang *et al.* (2008). According to this criterion, for three hundred steps, the variation of the mass flow at the inlet was less than 0.001 kg/s. The inlet and outlet mass flowrate difference was less than 0.5 percent. The adiabatic efficiency variation at per hundred steps was less than 0.3 percent. In this study, the similar convergence criterion was applied numerically for the stall initiation.

Table 2 Values of Y+ for different surfaces

Surfaces		222000 Grids	445000 Grids	780000 Grids
Hub	y_{min}^+	0.18	0.08	0.02
	y_{ave}^+	4.4	1.86	0.82
	y_{max}^+	8.01	4.5	1.44
Shroud	y_{min}^+	0.94	0.38	0.21
	y_{ave}^+	3.52	1.86	1.38
	y_{max}^+	7.36	3.97	1.6
Pressure Side	y_{min}^+	0.24	0.15	0.02
	y_{ave}^+	5.57	1.90	0.89
	y_{max}^+	10.95	4.38	1.65
Suction Side	y_{min}^+	0.23	0.08	0.01
	y_{ave}^+	4.41	1.77	0.76
	y_{max}^+	8.14	3.74	1.40

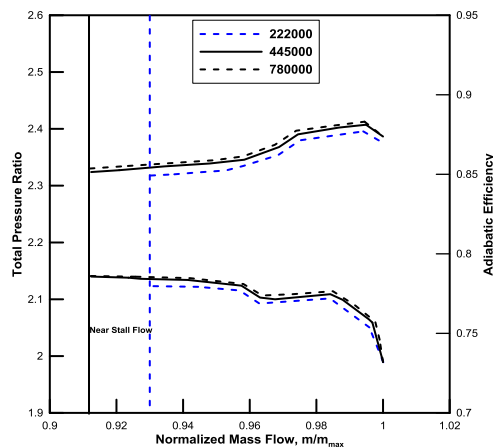


Fig. 4. Computational grids effect on compressor characteristic map

5. RESULT AND DISCUSSION

First of all, one passage steady simulations were performed on NASA Rotor 37 with smooth wall casing treatment for the purpose of comparison with the calculation of casing treatment afterward. The smooth wall casing treatment was compared with the experimental data of the AGARD Advisory Report which was reported by Dunham (1998). The numerical result data showed good correspondence with the tested data of rotor 37 for total pressure ratio and adiabatic efficiency and it is depicted in Fig. 6. Basically, the method of casing grooves in an axial flow compressor is used for the performance and stability improvement. To quantify the stability and performance of the compressor, the adiabatic

efficiency and SM parameters were used in this paper and the parameters are explained as follow.

$$SM = \left(\frac{\dot{m}_{peak}}{\dot{m}_{stall}} \times \frac{PR_{stall}}{PR_{peak}} - 1 \right) \times 100 \% \quad (1)$$

$$\eta_{peak} = \frac{\left(\frac{P_{t,out}}{P_{t,in}} \right)^{\frac{\gamma-1}{\gamma}} - 1}{\left(\frac{T_{t,out}}{T_{t,in}} \right) - 1} \quad (2)$$

Where PR and \dot{m} is the total pressure ratio and mass flow rate, and stall and peak subscripts denotes the adiabatic efficiency at peak & near to point of stall correspondingly. P_t , T_t , and γ represents total pressure, total temperature and specific heat ratio respectively.

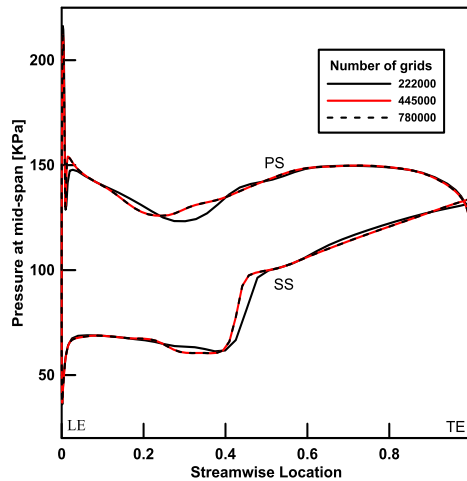


Fig. 5. Grid dependency test.

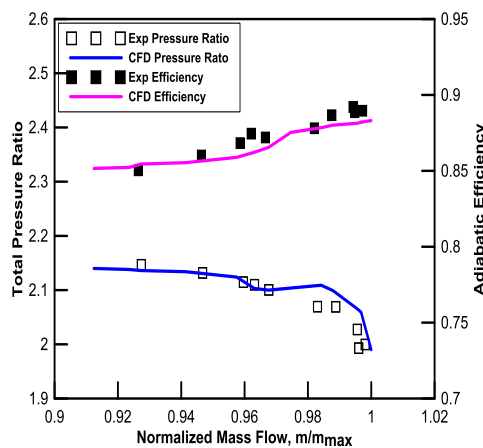


Fig. 6. NASA Rotor 37 validation, Total pressure ratio & Adiabatic Efficiency.

5.1 Performance Improvement by application of CGCT

TLV and flow at tip leakage leads to stagnation region and it goes to the passage shock downstream due to small mass flowrate, due to this reason vortex

breakdown occurred. It advances to severe blockage in the region of main flow ensuing instability in the axial flow compressor. The TLV breakdown is a general phenomenon in NASA Rotor 37 transonic axial flow compressor (Huang *et al.*, 2008; Du *et al.*, 2013). Model 1 of the rectangular shape of grooves was selected the basic model for this research to investigate the influence of CGCT on the performance and stability of axial flow compressor and was compared with smooth wall casing. Performance parameters for compressor were adiabatic efficiency, total pressure ratio, and stall margin. The close stall points for smooth wall casing and model 1 were 0.912 and 0.908 and is depicted in Fig. 7. The total pressure ratio for the smooth wall casing and model 1 near to stall points were 2.14 and 2.17 respectively. For model 1 the total pressure was a little bit higher than the smooth wall casing. This discrepancy is reported by many researchers (Beheshti *et al.*, 2004; Huang *et al.*, 2008). Adiabatic efficiencies for smooth wall casing and model 1 were 88.31 % & 88.11 % and the efficiency was much higher than efficiencies presented by Kim *et al.*, 2012; Mirzabozorg *et al.*, 2017). The efficiency for model 1 was less decreased than the smooth wall because only three grooves were installed between eighteen percent to fifty-eight percent and there was no groove installed in the leading and trailing edge and the groove locations among these places were more effective. The role of CGCT added a substantially minimizing mass flow near to stall point as compared to smooth wall casing and the stall margin was improved due to this reason. Higher efficiency and total pressure ratio could be achieved in the peak region by the installation of CGCT but there was a small reduction in the adiabatic efficiency over the entire flux range. So, the separation at the blade pressure surface which was formed due to pressure loss could reduce by CGCT momentum flux. As indicated in Fig. 8, It was observed that there was a pressure difference change among suction and pressure surface at every location of the grooves due to the fixing of grooves. It is depicted in Fig. 8 that the large pressure difference could be seen from eighteen to sixty percent of the blade chord. There are two significant impacts by installing the CGCT. One is the pressure fluctuation on the pressure surface that cause the increase of local pressure like a wave. Another is the downward movement of the shock wave that can be seen from the pressure distribution on suction surface which probably benefit the compressor stability. So, the consequences of installing CGCT are the increased of load and shock wave moving into the passage, both of which lead to increasing the pressure ratio and decreasing the flux ratio at stall point. The blockage was reduced in the location of the groove arises on the blade at the pressure surface as depicted in Fig. 9. A streamlines contour is shown in Fig. 9. It could be seen in Fig. 9(a) that the separation of the flow occurred at the leading edge of the pressure surface. Due to this separation the local spillage LE phenomena occurred. Basically, at the blade leading edge near the pressure surface, the low fluid region is caused the TLF (blockage at LE) which is linked to stall inception. This separation is suppressed with the help of CGCT as shown in Fig. 9(b). It could be

observed in Fig. 9(b) that the separation is suppressed at the leading edge of the blade pressure surface with the installation of CGCT. Large momentum flux is created on the pressure surface to the blade suction surface. Due to stippled separation at the blade pressure surface, it helped in enhancement on the performance and operating stability of the axial flow compressor.

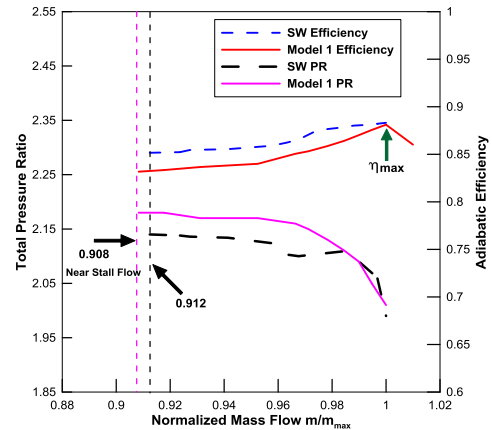


Fig. 7. Adiabatic efficiency & total pressure ratio performance curve for Smooth wall and Model 1.

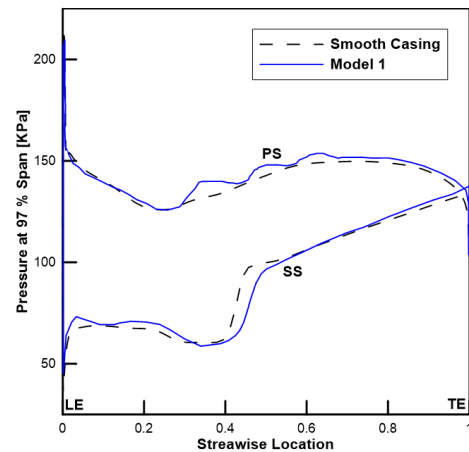


Fig. 8. Streamwise distribution of Pressure at 97 percent span (near stall point).

5.2 Influence of the CGCT with Several Shapes on Axial Compressor Performance

The performance of an axial flow compressor with different CGCT shapes is depicted in Fig. 2. The peak adiabatic efficiency and stall margin for each CGCT model are depicted in Figs. 10 and 11. The adiabatic efficiencies for all the models are a little bit decreased with the installation of the CGCT. The smooth wall casing shows the maximum adiabatic efficiency of 88.31 percent in Fig. 10. In comparison with smooth wall casing, the adiabatic efficiency for each model is decreased by 0.20 percent, 0.33 percent and 0.28 percent for all models respectively. As there is a little difference in the efficiency of smooth wall casing and all the three models. According to the author the grooves were only

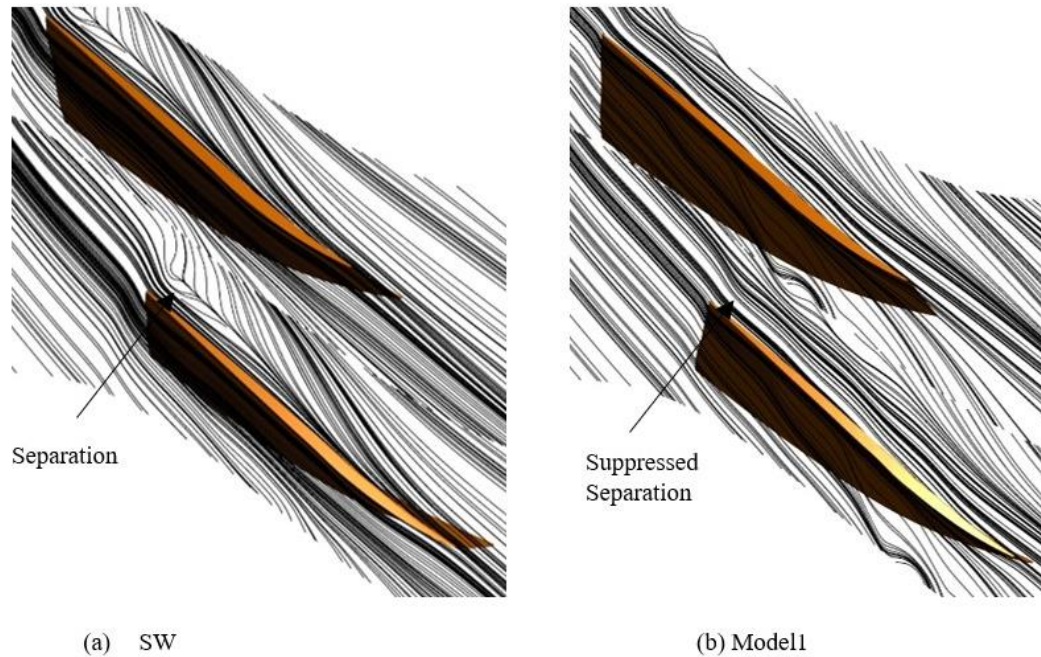


Fig. 9. Contours of streamlines at 98 percent span (near stall point) for (a) Smooth wall & (b) Model 1.

installed at the axial location of eighteen to fifty-eight percent of the blade chord as the grooves were very effective in the mentioned locations, hence there was a small difference in the efficiencies of all models with the smooth wall casing. All the models had a greater impact on the stall margin of the compressor as depicted in Fig. 11. Among all the three models only model 2 gave less stall margin than the other two models however, it gave a higher stall margin than the smooth wall casing. This stall margin is higher than what has been reported by Huang *et al.* (2008) and Kim *et al.* (2012). As seen in Fig. 11, model 1 showed 19.44 percent of the stall margin as compared to smooth wall casing and the stall margin was improved by 6.17 percent. For the other two models, the stall margins were also improved by 2.63 percent and 3.29 percent respectively. It is believed that the first and second groove which were installed at eighteen and thirty-eight percent of the blade chord gave more contribution to increased the stall margin while the last groove gave less contribution to increasing the stall margin of the compressor. According to the author, all the three CGCT (rectangular, chamfer and fillet) models have a good impact on the extension and enhancement of operating stability in the axial flow compressor.

Entropy contours for the smooth wall casing and other three models of CGCT at 99 % span (near stall point) are depicted in Fig. 12. It is clear from Fig. 12 that all the models had a maximum value of entropy at the blade tip. In the downstream region, all the models showed lower values for entropy with the application of CGCT except the smooth wall casing and the same is reported by Kim *et al.*, (2012) and Mao *et al.* (2018). This reduction of entropy generation shows the enhancement of the TLV

structure. The entropy value is lower in all the three models after the last groove because in the downstream there is no groove installed to tackle the TLV. By the installation of CGCT, the efficiency is recuperated in the region of low flow mass due to the lower value of the entropy initiation. Figure 12(b) showed lower entropy value in the downstream region than the other models and the reduction of entropy generation much improved the TLV in model 1 as compared to other models. More efficiency is recovered in the lower region for model 1. There is also a lower entropy value for model 3 in Fig. 12(d) but the entropy value is greater than model 1 and lower than model 2. According to author the efficiency is also recuperated for model 3 and reduced the TLV but the efficiency recovery of model 3 is smaller than model 1 and greater than model 2. Model 2 is more efficient than the smooth wall casing due to the reduction of TLV. It could be concluded that model 1 is the more effective model among all the models and the stall margin is much higher than the other models due to improved TLV in the low mass region and more efficiency recuperation.

Axial velocity contours for the normal shroud and other models of CGCT at 99 % span (near stall point) are depicted in Fig. 13. In transonic axial flow compressor when the rate of mass flow is decreased, the interaction intensity between the TLV and shock wave increased which leads to downstream to the low-speed zone in which there is loss of energy flow in the passage shock Du *et al.* (2013). The low-speed zone is called the region of the vortex stagnation zone. The region of vortex stagnation changes the direction of the main flow by augmenting pressure from the backside due to which separation occurred and the flow velocity decreased. But according to

some reports (Huang *et al.*, 2008; Kim *et al.*, 2012), the vortex stagnation zone can be reduced with the installation of CGCT. This shows that CGCT's is more useful for enhancing of the stability and operating range of the axial flow compressor. It is depicted in model 1 of Fig. 13 that vortex stagnation is more enhanced than model 2 and 3 because the rectangular grooves of model 1 are more capable to reduce the blockage zone. It is concluded that the model 1 is the best model in terms of stability and operating range as compared to the other two models. As depicted in Fig. 13 model 3 is more enhanced than model 2 because there is more improvement in the vortex stagnation zone due to reduced blockage zone. However, model 2 is less enhanced compared to model1 and model 3 due to less improvement of vertex stagnation zone, even though model 2 has more stall margin and stable operating range than that of the smooth wall casing. In Fig. 13(a) the value of axial velocity is higher at the blade tip after the mid-chord of the blade while the dissimilar pattern is observed in all the three models which indicates the improvement in the stall margin and performance of the axial flow compressor.

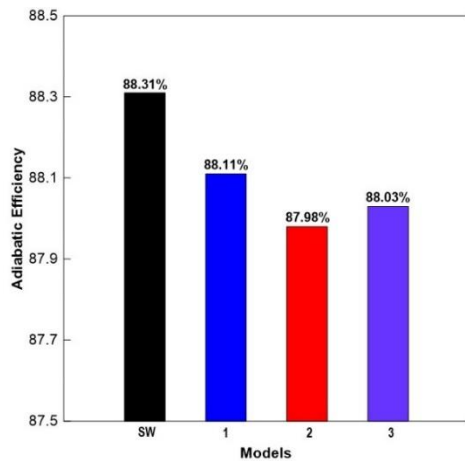


Fig. 10. Adiabatic efficiency comparison of different models.

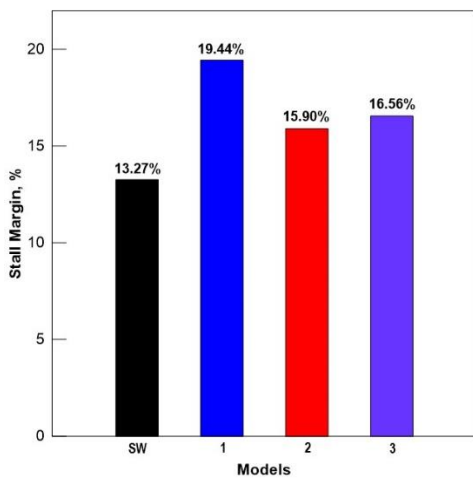


Fig. 11. Stall margin comparison of different CGCT models.

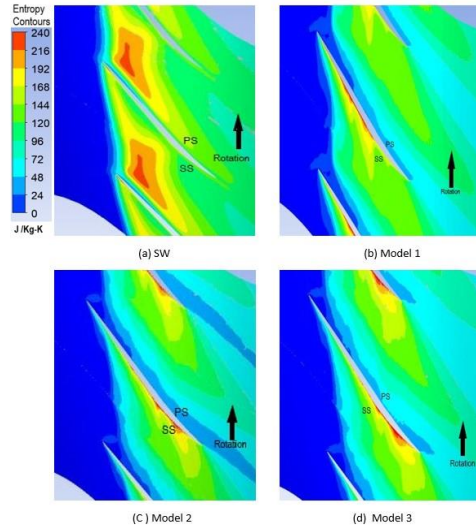


Fig. 12. Entropy contours at 99 percent (near stall point) (a) Smooth wall, (b) model 1, (c) model 2 & (d).

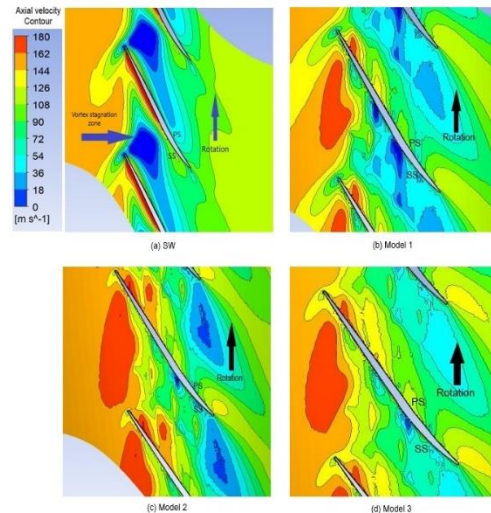


Fig.13. Axial velocity contours at 99 percent span (near stall point) (a) smooth wall, (b) model 1, (c) model 2 & (d) model 3.

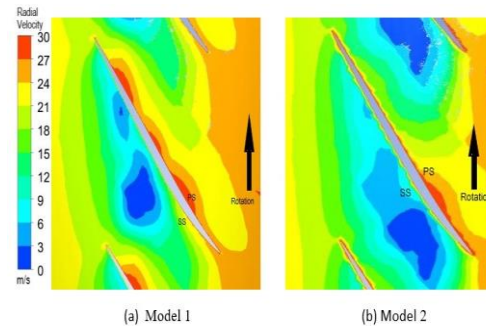


Fig. 14. Radial velocity contours at 99 percent span (near stall point) (a) model 1 & (b) model 2.

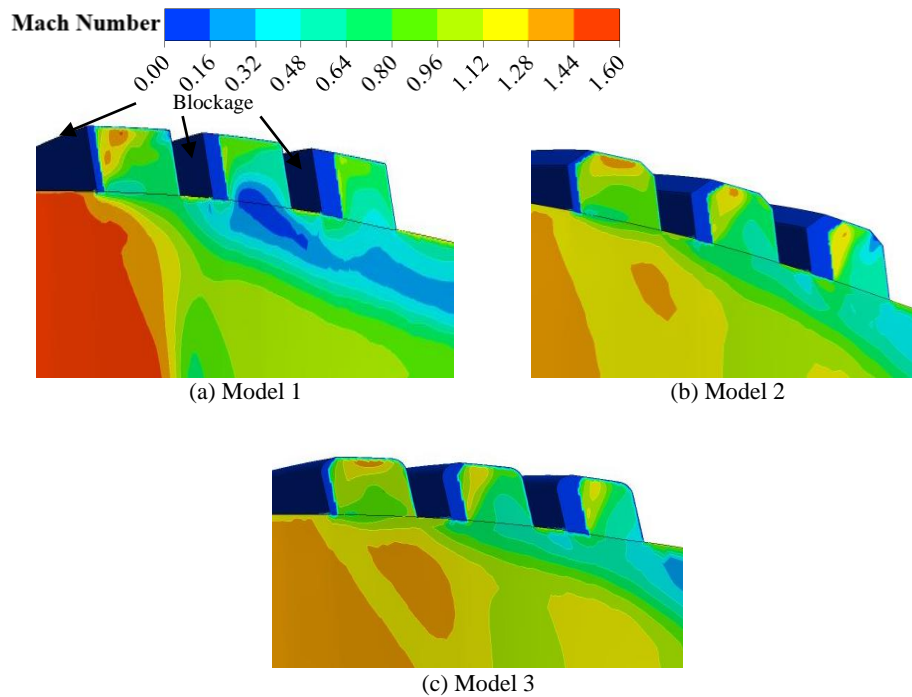


Fig. 15. Mach number contours of CGCT near stall point for (a) model 1, (b) model 2 & (c) model 3.

The radial velocity contour for model 1 and 2 is depicted in Fig. 14. When comparing the radial velocity of model 1 and 2, it was found that model 1 is more effective than model 2 in term of stall margin and efficiency. The leakage of flow to the grooves started from the blade pressure surface and at the suction surface of the blade and is injected itself, beyond this the flow is mixed up with the main flow and the combined flow is going downstream which is also reported by *Khan et al. (2011)*. It is believed that due to the location of first and second groove, which are installed at eighteen and thirty-eight percent of the blade chord respectively, the power of leakage flows slowly decreases. It is found that the last groove which was installed in downstream (fifty-eight percent of the blade chord) had a little impact on flow enclosure and the improvement of stall margin. It is proposed that the best locations for the two grooves are in between eighteen to thirty-eight percent of blade axial chord location. It can be seen in Fig. 14 that there is more blockage generated in model 2 due to additional mixed up of the main flow and the tip flow than model 1 and there is reduced TLV in the model 1 near the leading edge of the blade. This reduced TLV shows enhancement in axial flow compressor stability. It is noteworthy that model 2 gave better stability and stall margin than the smooth wall casing and as shown in Fig. 11.

Mach number contour is shown in Fig. 15 for all the three models. As depicted in Fig. 15(a) maximum Mach number is recovered in the first and second grooves and the first two grooves suppressed more blockage of the TLV. The impact of the last groove is small. The first two grooves give more benefit to the stall margin. In model 2 the flow field is different

from model 1. Mach number is recovered in the middle of the first groove while the same pattern is not observed in model 1. The second and third groove give maximum Mach number in the chamfer region and the contribution of the first two grooves to stall margin is more as compared to the last groove. Additionally, the last groove shows more blockage as compared to the first two grooves. The flow field in model 3 is totally different from model 1 and model 2. Maximum Mach number is observed in the middle of the first groove, while the second and third grooves give high Mach number near the fillet region and there is no additional blockage observed in the third groove. All the models have a positive impact on the stall margin and stability of the compressor, but model 1 gives more stall margin than the other two models as shown in Fig. 11.

CONCLUSION AND OUTLOOK

This study investigated numerically the influence of the three grooves CGCT on the Adiabatic efficiency and stall margin using RANS three-dimensional equation. Following are the findings of this numerical research work.

- (1) The interaction intensity between the TLV and shock wave produced a vortex stagnation zone which caused instability in axial flow compressor. The vortex stagnation zone had a greater impact on the stall. It was also found that the separation from the pressure surface of the blade leading edge had a substantial impact on the initiation of the stall in the compressor.
- (2) The vortex stagnation zone was decreased by the installation of CGCT. The installation of

CGCT decreased the tip clearance flow which helped to reduce the vortex stagnation zone and is useful to maximize the stability and performance of axial flow compressor.

- (3) It was observed in the simulations that the first two grooves in all models gave substantial improvement to the stall margin while the last groove in all models had a small impact on the stall margin of the axial flow compressor.
- (4) The flow field enhancement for chamfer and fillet models were observed at the blade tip according to the Mach number and axial velocity contours. The installations of chamfer and fillet corners type CGCT suppressed the TLF which were beneficial for the stall margin improvement.
- (5) The axial flow compressor performance and stability were changed with various types of CGCT geometry. In comparison among the three types of grooves, the rectangular shape was the best one while the fillet shape is relatively better than the chamfer type in terms of efficiency and stall margin.
- (6) The maximum stall margin and efficiency were achieved with a rectangular shape and the stall margin and efficiency were 19.44 and 88.11 percent respectively. The performance of the rectangular shape was better than the other two models.
- (7) With the application of CGCT, the maximum adiabatic efficiency was slightly decreased. The CGCT generated the entropy due to corner separation and mixed with reverse TLF to reduce the adiabatic efficiency of the compressor.
- (8) The three grooves were located from eighteen percent to fifty-eight percent of the blade chord. The location of the first, second and third groove were eighteen, thirty-eight. In these locations, the grooves reduced the blockage region of TLV more effectively and increased the performance and stability range of the axial flow compressor.

To understand the further mechanism of CGCT could be designed by optimizing the shapes of the rectangular grooves with fillet and chamfer edges.

REFERENCES

- ANSYS (2017). ANSYS CFX-solver theory guide, Release, ANSYS Inc.
- Bailey, E. E. (1972). *Effect of grooved casing treatment on the flow range capability of a single-stage axial-flow compressor*. Washington, United States
- Beheshti, B. H., J. A. Teixeira, P. C. Ivey, K. Ghorbanian and B. Farhanieh (2004). Parametric study of tip clearance-casing treatment on performance and stability of a transonic axial compressor. *49th International Gas Turbine and Aeroengine Congress and Exhibition*, Vienna, AUSTRIA.
- Dinh, C. and K. Kim, K. (2017). Effects of Non-axisymmetric Casing Grooves Combined with Airflow Injection on Stability Enhancement of an Axial Compressor. *International Journal of Turbo & Jet-Engines* 2016-0077.
- Du, J., F. Lin, J. Chen, C. Nie and C. Biela (2013). Flow structures in the tip region for a transonic compressor rotor. *Journal of turbomachinery* 135(3), 031012.
- Dunham, J. (1998). *CFD validation for propulsion system components* (la validation CFD des organes des propulseurs): Advisory Group for Aerospace Research and Development Neuilly-Sur-Seine, France.
- Hah, C. (2018). The Inner Workings of Axial Casing Grooves in a One and a Half Stage Axial Compressor with a Large Rotor Tip Gap: Changes in Stall Margin and Efficiency. *Proceedings of ASME Turbo Expo 2018 Turbomachinery Technical Conference and Exposition GT2018*, 11-15, Oslo, Norway.
- Hah, C., D. C. Rabe and A. R. Wadia (2004). Role of tip-leakage vortices and passage shock in stall inception in a swept transonic compressor rotor. *Proceedings of ASME Turbo Expo 2004 Power for Land, Sea, and Air* 14-17, Vienna, Austria.
- Houghton, T. and I. Day (2011). Enhancing the stability of subsonic compressors using casing grooves. *Journal of Turbomachinery* 133(2), 021007.
- Huang, X., H. Chen and S. Fu (2008). CFD investigation on the circumferential grooves casing treatment of transonic compressor. *Proceedings of ASME Turbo Expo 2008: Power for Land, Sea and Air GT2008* 9-13, Berlin, Germany.
- Khan, J., K. Parvez, S. Ahmad and A. Mushtaq (2011). Effect of circumferential grooves and tip recess on stall characteristics of transonic axial compressor rotor. *49th AIAA Aerospace Sciences Meeting including the New Horizons Forum and Aerospace Exposition* 4-7, Orlando, Florida
- Kim, J., K. Choi and K. Kim (2012). Performance evaluation of a transonic axial compressor with circumferential casing grooves. *Proceedings of the Institution of Mechanical Engineers, Part A: Journal of Power and Energy* 226(2), 218-230.
- Lang, J., W. Chu, H. Zhang, S. Ma and X. Chen (2017). Investigation of In-Stall Behavior in a Transonic Compressor Rotor. *Proceedings of ASME Turbo Expo 2017: Turbomachinery Technical Conference and Exposition GT2017* 26-30, Charlotte, NC, USA.
- Mirzabozorg, M. A. S., M. Bazazzadeh and M.

- Hamzade (2017). Numerical study on the effect of single shallow circumferential groove casing treatment on the flow field and the stability of a transonic compressor. *Journal of Applied Fluid Mechanics* 10(1), 257-265.
- NUMECA International (2009). *IGG v8.9-1 and Autogrid5 v8.9-1, User Manual*, NUMECA International, Brussels.
- PTC Creo Elements Pro 5.0 M220 Win64.
- Rabe, D., and C. Hah (2002). Application of casing circumferential grooves for improved stall margin in a transonic axial compressor. *the ASME Turbo Expo 2002: Power for Land, Sea, and Air*. 3-6, Amsterdam, The Netherlands.
- Rolfes, M., M. Lange and K. Vogeler (2015). Experimental investigation of circumferential groove casing treatments for large tip clearances in a low speed axial research compressor. *Proceedings of ASME Turbo Expo 2015: Turbine Technical Conference and Exposition GT2015* 15–19, Montréal, Canada.
- Mao et al. (2018). The impact of casing groove location on the flow instability in a counter-rotating axial flow compressor. *Journal Aerospace Science and Technology* 76 (2018) 250–259.
- Sakuma, Y., T. Watanabe, T. Himeno, D. Kato, T. Murooka and Y. Shuto (2014). Numerical analysis of flow in a transonic compressor with a single circumferential casing groove: influence of groove location and depth on flow instability. *Journal of turbomachinery*, 136(3), 031017.
- Schlechtriem, S. and M. Lötzerich (1997). Breakdown of tip leakage vortices in compressors at flow conditions close to stall. *the Interational Gas Turbine & Aeroengine Congress & Exhibiton 197 Orlando Florida*.
- Shabbir, A. and J. J. Adamczyk (2005). Flow mechanism for stall margin improvement due to circumferential casing grooves on axial compressors. *Journal of turbomachinery* 127(4), 708-717.
- Song, W., Y. Zhang and H. Chen (2018). Design and Optimization of Multiple Circumferential Casing Grooves Distribution Considering Sweep and Lean Variations on the Blade Tip. *Energies* 11(9), 2401.
- Suder, K. L. and M. L. Celestina (1994). Experimental and computational investigation of the tip clearance flow in a transonic axial compressor rotor. *39th International Gas Turbine and Aeroengine Congress and Exposition sponsored by ASME*, 13-16 The Hague, Netherlands.
- Wilke, I., and H. P. Kau (2002). A numerical investigation of the influence of casing treatments on the tip leakage flow in a HPC front stage. *Proceedings of ASME Turbo Expo* 3–6, Amsterdam, The Netherlands.
- Yamada, K., K. Funazaki and M. Furukawa (2007). The behavior of tip clearance flow at near-stall condition in a transonic axial compressor rotor. *Proceedings of GT2007 ASME Turbo Expo: Power for Land, Sea and Air* 14-17, Montreal, Canada.